Single Image Dehazing based on Additive Wavelet Transform

Nur Huseyin Kaplan

***Abstract*—In this work, a single image dehazing method which uses the multi-scale products of additive wavelet transform as a prior is presented. In this method, first, the additive wavelet transform is applied to the hazy image to obtain its approximation and wavelet layers. Then the multi-scale products of the approximation and detail layers of the input hazy image are calculated. The multi-scale products of approximation and wavelet layers are summed up to obtain the proposed prior. Observations demonstrate that the proposed prior calculation keeps the detail information of the image, while detecting the haze. Using the proposed prior and commonly used hazy image model together, an efficient dehazing method is constructed. The comparisons between the proposed method and commonly used dehazing methods show that the proposed method has better dehazing performance than the traditional methods.**

***Index Terms*—Dehazing, Defogging, Additive wavelet transform.**

I. Introduction

IMAGING SYSTEMS tend to construct low contrast images especially in bad weather conditions like fog and haze. The low visibility of these image is dependent on the scattering and absorbing of the light by the particles within the atmosphere. Since, most of the automated systems and advanced image processing algorithms need higher contrast images, dehazing is an important problem for these applications.

Since, the amount of the haze depends on the distance between scene and the imaging device, the depth information of these images are not present. Therefore, image dehazing is a challenging problem because of the unknown depth information. The traditional enhancement methods, like histogram based methods are not capable of restoring the depth of the images [1], [2], [3].

In order to increase the performance of dehazing algorithms, multiple images of the same scene taken under different weather conditions are used[4], [5], [6]. These algorithms are effective for haze removal, however the need of the multiple scenes for input is generally not possible.

In recent years, many single image dehazing algorithms have been developed [7], [8], [9], [10], [11], [12], [13], [14], [15], [16]. These methods generally use a prior or assumption alongwith the common hazy image model.

Tan et al. [7] proposed a method to improve the local contrast of the hazy images under the assumption that haze free images have higher contrast. However, the haze free images are not always higher in contrast, this method distorts the color information of the input images. Fattal [9] proposed a dehazing algorithm based on Independent Component Analysis (ICA). This method produces better results than Tan's method, however, the method is developed for only color images and does not work well for heavy hazed images.

He et al. [8] proposed to use the Dark Channel Prior (DCP) for dehazing. The prior calculates the darkest pixel within a patch, based on the observation that at least one pixel has low intensity for at least one color channel. Although being an effective method, it distorts the color, especially in the sky region and the time consumption is too high due to the soft matting process to reduce the effects caused by patches. In [14], the shortcomings of DCP have been investigated, and a dehazing method based on bright object handling is proposed.

Zhu et al. [13] has proposed a colour attenuation prior for image dehazing with a supervised learning process.

In recent years, dehazing methods based on decomposition [17] and fusion [18] strategies have also been proposed. Moreover, many learning algorithms [19], [20] are also used for dehazing purposes. Cai et al. [15] has proposed a trainable system (DehazeNet) to estimate the transmission with the help of convolutional neural networks.

Recently a multi-scale products prior based method (MP) has been proposed [16]. In this method, the input hazy image is decomposed by an undecimated Laplacian decomposition to obtain its detail and approximation subbands. Then, the multi-scale product of the approximation subband is used to calculate the prior. This prior is capable of removing the haze, as well as it does not distorts the color in the sky region. However, the method can not remove the haze especially in the mid regions. In addition, the method can only be applicable for color images.

Motivated by the results obtained in [16], an additive wavelet transform based method is proposed in this paper. The proposed method decomposes the input image to obtain the approximation and wavelet layers with additive wavelet transform. The proposed method takes into consideration both the approximation and wavelet layers to obtain the prior. Based on the proposed prior and the commonly used hazy image model, an effective dehazing algorithm is developed.

A large dataset of hazy image has been used to examine the proposed method. The resulting images demonstrate that the proposed dehazing algorithm produces images that have higher contrast and visibility. Moreover, the proposed method does not have the distortions of the traditional methods, as well as it is more efficient than the MSP method for mid regions.

Rest of the paper is as follows. An explanation of the additive wavelet transform is given in Section II. The proposed

Nur Huseyin Kaplan is with the Department of Electrical and Electronic Engineering, Engineering and Architecture Faculty, Erzurum Technical University, Erzurum, 25050 TURKIYE e-mail: huseyin.kaplan@erzurum.edu.tr
orcid ID: 0000-0002-4740-3259
Manuscript received Jun 08, 2022; accepted Dec 16, 2022. DOI: 10.17694/bajece.1127633

dehazing method is given in Section III. The comparisons of the proposed method with traditional methods are included in Section IV. The paper is concluded in Section V.

II. Additive Wavelet Transform

Additive Wavelet Transform (AWT) has a wide area of use in image processing applications such as pansharpening [21], because of its shift-invariance property. In this transform, first an approximation layer is obtained by filtering the input image (I) with a bicubic spline filter

$$I_1 = I * h_1 \tag{1}$$

where, I_1 is the first approximation layer and the bicubic spline filter h_1 can be given as:

$$h_1 = \begin{bmatrix} 1 & 4 & 6 & 4 & 1 \\ 4 & 16 & 24 & 16 & 4 \\ 6 & 24 & 36 & 24 & 6 \\ 4 & 16 & 24 & 16 & 4 \\ 1 & 4 & 6 & 4 & 1 \end{bmatrix} \tag{2}$$

The difference between the approximation layer and the input image gives the first wavelet layer.

$$W_1 = I - I_1 \tag{3}$$

For further decomposition, the first approximation layer is filtered again as

$$I_2 = I_1 * h_2 \tag{4}$$

Here, I_2 is the 2 nd level approximation layer, h_2 is the 2 nd level bicubic spline filter, which is obtained by doubling the size of h_1 by filling the gaps with zeros. The 2 nd level detail layer can be obtained as:

$$W_2 = I_1 - I_2 \tag{5}$$

To obtain the approximation and details layer of l th level, the equations are generalized as

$$I_l = I_{l-1} * h_l \tag{6}$$

$$W_l = I_{l-1} - I_l \tag{7}$$

The original image can be reconstructed by:

$$\hat{I} = I_L + \sum_{i=1}^{L} W_i \tag{8}$$

where L is the level of decomposition.

III. The Proposed Dehazing Method

Commonly used hazy image model can be given as [9], [16], [22], [23]:

$$I_m(x) = J_m(x)t(x) + A_m[1 - t_m(x)], m = R, G, B \tag{9}$$

where $I_m(x)$ and $J_m(x)$ are the m th band of the input hazy and haze free images, respectively. A_m is the m th band airlight, while $t_m(x)$ is the transmission of the m th band, which describes the unscattered data.

By using (7), $J_m(x)$ can be determined by using the following equation.

$$J_m(x) = \frac{I_m(x) - A_m[1 - t(x)]}{t(x)} \tag{10}$$

In order to obtain the haze free $J_m(x)$ image, the unknown airlight A_m and the transmission $t(x)$ should be estimated.

A. The Proposed Prior

In MP method described in [16], the prior has been obtained by the multi-scale products of the approximation subbands of the undecimated Laplacian decomposition. Moreover, a single prior is obtained for the color image.

In this work, the proposed prior is obtained by the use of both approximation and wavelet layers of the AWT. In addition, priors for every band of image is calculated separately.

In order to obtain the proposed prior, first the approximation and wavelet layers of the input hazy image are calculated by applying the AWT to the each color band of the image. The approximation layers are calculated as:

$$I_l^m = I_{l-1}^m * G_l^m \tag{11}$$

where $m = R, G, B$ is the color band of the image and $l = 1, 2, ..., L$ is the level of decomposition. I_l^m is the l th level approximation layer of the m th band.

The wavelet layers are obtained by the following equation.

$$W_l^m = I_l^m - I_{l-1}^m \tag{12}$$

where W_l^m is the l th level wavelet layer of m th band.

Then, approximation multi-scale product for each band is calculated by multiplying adjacent approximation layers.

$$MSP_I^m = I_1^m I_2^m ... I_L^m \tag{13}$$

and the wavelet multi-scale product for each image band is obtained by multiplying the adjacent wavelet layers.

$$MSP_W^m = W_1^m W_2^m ... W_L^m \tag{14}$$

If a pixel value at a certain location is higher, corresponding pixel value at adjacent layer is higher too, and vice versa [24]. Multiplying adjacent layers to calculate multi-scale products may dilute redundant information and emphasize the important information of the image [24].

Finally, the proposed additive wavelet prior (AWP) for the m th band is calculated as:

$$AWP_m = \sqrt[L]{MSP_I^m + MSP_W^m} \tag{15}$$

In (15), the calculated wavelet and approximation multi-scale products are summed up. By this way, the priors calculated separately for each band, which makes the proposed method to be applicable for gray scale images as well. Including the wavelet layers in the summation makes the prior to keep detail information.

The flowchart of the calculation of proposed prior is given in Fig.1.

In order to determine the decomposition level, the effect of the levels on the prior is given in Fig.2.

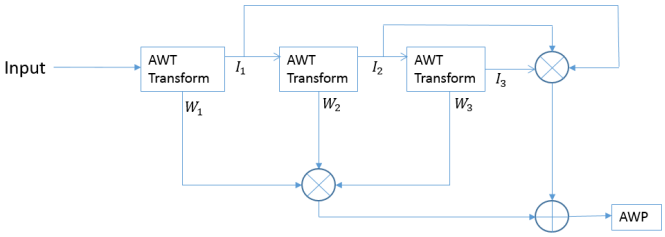

Fig. 1. Flowchart for the proposed AWP.

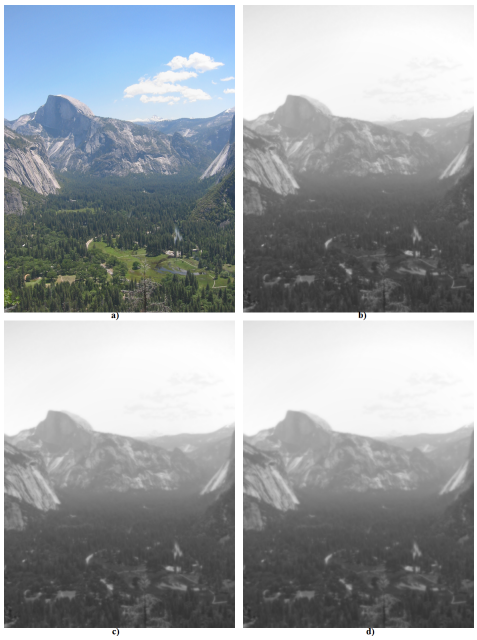

Fig. 2. a) Input hazy image, the proposed AWPs obtained for b) 2 levels, c) 3 levels, and d) 4 levels of decomposition.

As seen in Fig.2, choosing the decomposition level higher than 2, the proposed prior tends to be blurry, which means that the prior is not able to keep important information of the image. Observing various hazy images, 2 levels of decomposition have been chosen.

Since, the proposed prior uses the approximation and wavelet layers together, the prior expected to keep both rough information and detail information of the input image. The proposed prior is used to estimate transmission, therefore by the use of this prior, a better transmission is expected to be obtained.

B. The Airlight and Transmission Estimates

The airlight estimation is equal to the mean of the brightest 0.1% pixels of the image as described in [8], [16].

For the estimation of the transmission, a similar way described in [8], [16] is followed. First, the hazy image is divided by the calculated airlight and proposed AWP of this normalized image is obtained. The calculated AWP is smoothed by the bicubic spline filter. The equation for transmission calculation can be formulated as:

$$t_m(x) = 1 - \omega AWP(\frac{I_m}{A_m}) * h_1 \tag{16}$$

where, ω is the amount of the haze to be removed. A transmission estimate with the proposed prior is given in Fig.3.

The dehazed images with different ω values are given in Fig.4.

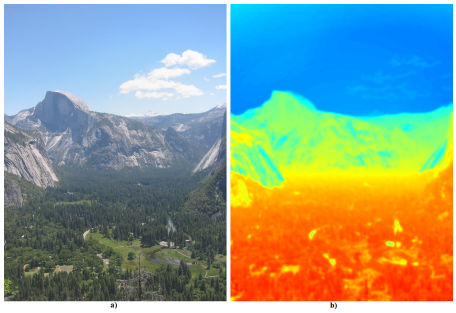

Fig. 3. a) Hazy image b) Transmission estimate with proposed AWP.

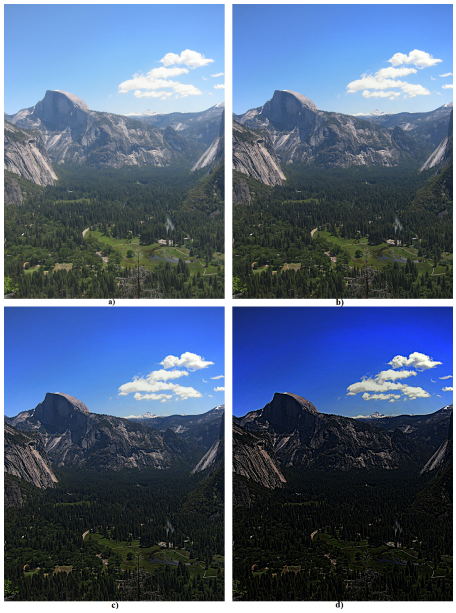

Fig. 4. Dehazed images for a) $\omega = 0.25$ b) $\omega = 0.5$, c) $\omega = 0.75$, d) $\omega = 0.9$

The transmission estimated for low ω values will result in too hazy images as seen in Fig.4.b, while high ω values will result in dark images as seen in Fig.4.d. Since, the transmission estimations obtained by the proposed prior is already similar to the image itself, no additional computation is needed to recover the dehazed image.

After observing different kinds of hazy images, ω value should be chosen around 0.75.

C. Reconstruction of the Haze Free Image

The haze free image can be recovered as:

$$J_m(x) = \frac{I_m(x) - A_m}{t_m(x)} + A_m \tag{17}$$

The proposed dehazing method can be summarized as follows:

1) The approximation and wavelet layers for the band of the hazy image are obtained by equations (11) and (12), respectively.
2) The multi-scale products for approximation and wavelet layers are calculated according to equations (13) and (14), respectively.
3) Obtained multi-scale products are summed up by (15) to obtain the proposed prior (AWP).
4) The airlight value for the corresponding band is obtained by the mean of the brightest 0.1% pixels of AWP.
5) The transmission is estimated by using the airlight and the proposed prior as in (16).
6) The haze free band of the input image is obtained by equation (17).
7) If the input image is a color image, above steps are repeated for the next color band of the image.

IV. Experimental Results

In order to understand the performance of the proposed AWP method, comparisons with the traditional methods are made. The proposed AWP and the classical methods are applied to a variety of hazy images. The comparisons are made both visually and quantitatively.

A. Visual Comparison

The first hazy image is shown in Fig.5.a. The dehazing results for Tan [7], Tarel [10], Kopf [6], DCP [8], Fattal [9], MP [16] and the proposed AWP method are given in Fig.5.b-h, respectively. According to Fig.5.b, Tan's method distorts the color for overall image. Fig.5.c shows that Tarel's method can not keep the color information, especially at the far end. Kopf's method, as seen in Fig.5.d, has a good performance for far scene, while it has a poor performance in closer regions. As seen Fig.5.f, Fattal's method has a poor performance where haze is thicker, as seen in the middle and far areas, even though it performs good for closer areas. As seen in Fig.5.e, DCP method distorts the color at the far end, especially in sky region, even though having a good performance in other regions. MP method as shown in Fig.5.g, does not distorts the color information and has a better performance than the aforementioned methods. However, a closer look demonstrates that the dehazing performance for middle area is not good enough. The proposed AWP method, as seen in Fig.5.h, has a better performance for overall image.

For further comparison, a scene from New York City that includes more details shown in Fig.6.a is used. The haze removal results for Tan [7], Tarel [10], Kopf [6], DCP [8], Fattal [9], MP [16] and the proposed AWP method are shown in Fig.6.b-h, respectively. Tan's method has distorted the colors as expected. Tarel's method has a poor performance for the far scene, while Kopf's method has a poor performance for the closer region. Fattal' s method can not dehaze the regions with thicker haze. DCP method overamplifies the sky region, while it can not amplify the right top of the scene. MP method being better than the former methods, can not dehaze the mid range of the image. The proposed AWP method has a better performance for the whole image.

In order to see the differences between the dehazing methods accurately, zoomed areas of Fig.6 is given in Fig.7. The zoomed version includes the sky region (far end) and mid range of Fig.6.

As seen in Fig.7, Tan' s, DCP method and Tarel's method distort the color of the sky. Moreover, under the sky region, the visibility has not increased for He's, Fattal and MP method. The best dehazing is performed by the proposed AWP method. A closer look to mid area demonstrates that, Tan' s and Tarel' s method suffers from color distortion. Kopf, DCP, Fattal and MP methods can not dehaze the mid range well. The proposed method dehazes the mid range and increases the visibility better than the former methods.

B. Quantitative Comparison

In order to make an objective comparison, the proposed AWP method is compared quantitatively with state of art methods. The figures used are given in [12], which are available online. Three of the figures and true transmissions are included in this paper for comparison purposes. Fig.8 shows the original haze-free images and dehazed images obtained by, Fattal[9], DCP[8], CL[12], Catt[13], DehazeNET[15] and AWP methods, respectively. According to the Fig.8, the dehazed images obtained by DCP, CL, and the proposed AWP methods are seems to be the closest to the original ones.

In order to compare quantitatively, SSIM and RMSE indexes are evaluated between the original image and dehazed images by the methods abovementioned. In addition, the RMSE values are calculated between the true transmission and recovered transmissions of the methods. The RMSE and SSIM values calculated between haze-free and dehazed images are given in Table 1.

TABLE I
Quantitative Comparison between haze-free and dehazed images

Figure	Metric	Fattal[9]	DCP[8]	CL[12]	Catt[13]	DehazeNET[15]	AWP
Mansion	RMSE(%)	10.3819	9.2994	**8.6000**	18.6304	13.0867	9.0765
	SSIM	0.8838	0.7241	**0.9013**	0.3334	0.4752	0.8909
Flower	RMSE(%)	3.2497	3.9622	**2.3262**	15.9957	10.2755	2.8838
	SSIM	0.8973	0.8940	**0.9099**	0.5964	0.5629	0.9030
Couch	RMSE(%)	8.6370	7.5886	7.6351	14.4420	13.8691	**7.1690**
	SSIM	0.8930	0.8944	0.8949	0.6615	0.6568	**0.9026**

According to Table 1, the best SSIM and RMSE values for Mansion and Flower images are obtained by CL method followed by the proposed method. CL method is slightly better than the proposed AWP method for this figures. For Couch

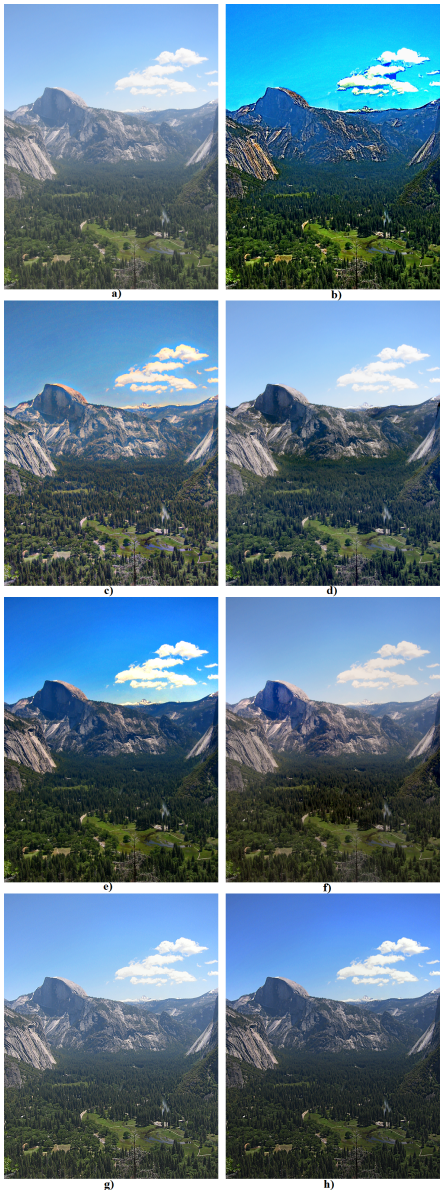

Fig. 5. a) Hazy image, Dehazing results for b) Tan c) Tarel, d) Kopf, e) DCP, f) Fattal, g) MP and h) the proposed AWP methods.

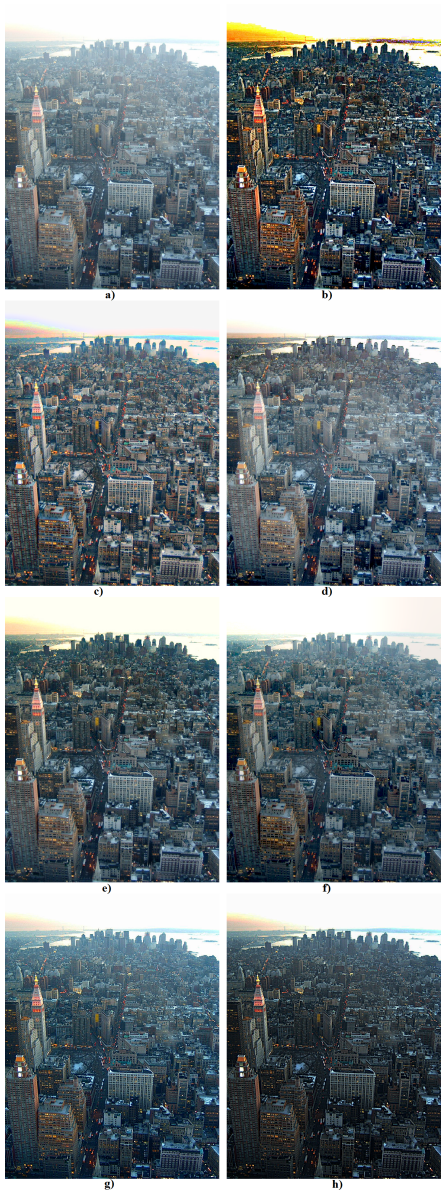

Fig. 6. a) Hazy image, Dehazing results for b) Tan c) Tarel, d) Kopf, e) DCP, f) Fattal, g) MP and h) the proposed AWP methods.

image, the best scores are obtained by the proposed AWP method.

For further comparison, recovered transmission of the methods aforementioned and the transmissions are given in Fig.9. According to Fig.9, the best recovered transmissions seems to be achieved by CL, DehazeNET and the proposed AWP methods.

The RMSE values calculated between true transmission and dehazing methods are given in Table 2.

TABLE II
RMSE VALUES BETWEEN TRUE TRANSMISSION AND RECOVERED TRANSMISSIONS

Figure	Fattal[9]	DCP[8]	CL[12]	Catt[13]	DehazeNET[15]	AWP
Mansion	25.9045	31.2422	18.0345	28.9952	**17.5627**	19.8263
Flower	52.7966	16.1832	**12.1464**	40.2297	23.9222	14.6925
Couch	27.6459	24.9502	25.6094	26.2958	25.3566	**23.8337**

According to Table 2, the best RMSE value for Mansion image is obtained by DehazeNET method followed by the proposed AWP and CL methods. For Flower image, the best score is achieved by CL followed by the proposed method. For Couch image, the best score is obtained by the proposed AWP method.

Experiments are performed in Matlab with a 2.4 GHz Intel i3 processor PC. The average running time of the methods are tabulated in Table 3. It can be seen that the proposed AWP method is nearly 30 times faster than the DCP method and 10 times faster than Catt method.

Taking into consideration both visual and quantitative comparisons, the proposed AWP method is either superior to the classical methods or in good agreement with the results of the state-of-art methods.

Fig. 7. A closer look to Fig.6. a) Hazy image, Dehazing results for b) Tan c) Tarel, d) Kopf, e) DCP, f) Fattal, g) MP and h) the proposed AWP methods.

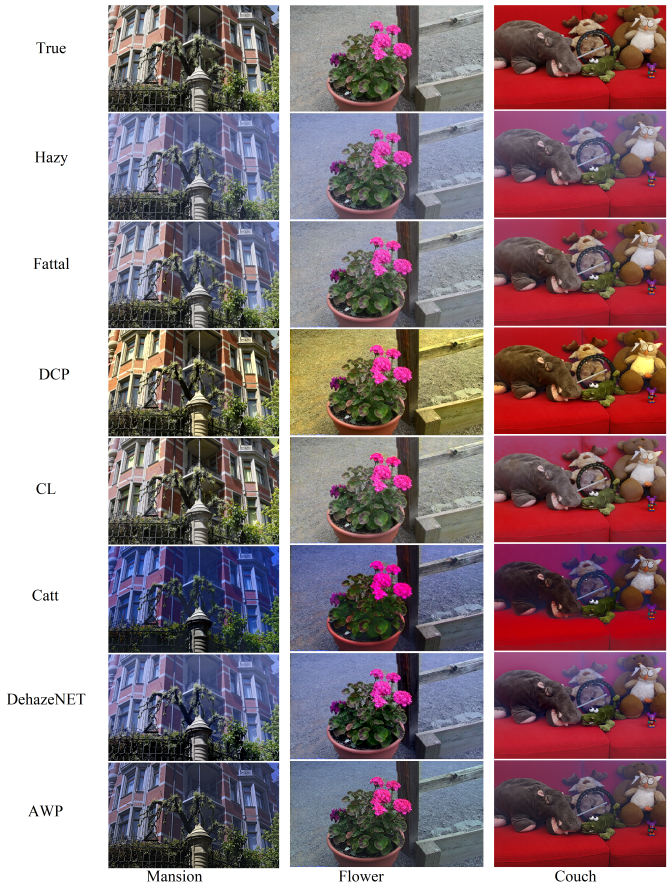

Fig. 8. Comparison with synthetic hazy images.

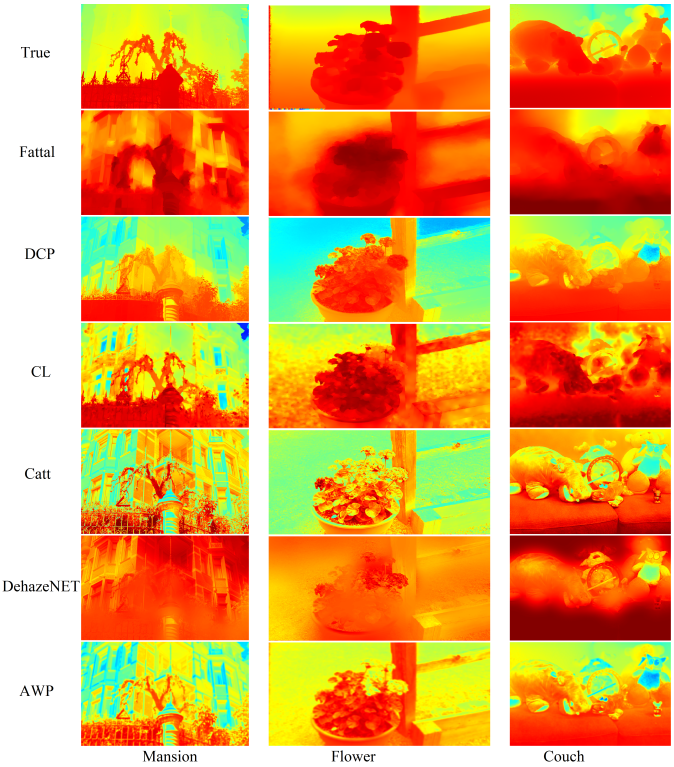

Fig. 9. Comparison of recovered transmissions with synthetic hazy images.

TABLE III
AVERAGE TIME CONSUMPTION OF THE METHODS FOR 1024X640 SIZED IMAGES

Method	Fattal[9]	DCP[8]	Catt[13]	DehazeNET[15]	AWP
Time Consumption (sec)	4.41	9.98	3.52	6.73	**0.32**

V. CONCLUSION

In this paper, a novel prior for single image dehazing is proposed. In order to obtain the proposed prior, first additive wavelet transform is applied to the hazy image to obtain the approximation and wavelet layers. The adjacent approximation and wavelet layers are multiplied and summed up to calculate the proposed prior. This new prior detects the haze present in the image, as well as it keeps the important details of the image. Using the proposed prior alongwith the commonly used hazy image model, an effective dehazing method is obtained. The visual and quantitative comparisons with traditional methods demonstrate that the proposed method outperforms the traditional methods.

REFERENCES

[1] T. K. Kim, J. K. Paik, and B. S. Kan, "Contrast enhancement system using spatially adaptive histogram equalization with temporal filtering," *IEEE Transactions on Consumer Electronics*, vol. 44, no. 1, pp. 82–87, 1998.

[2] J. A. Stark, "Adaptive image contrast enhancement using generalizations of histogram equalization," *IEEE Transactions on Image Processing*, vol. 9, no. 5, pp. 889–896, 2000.

[3] J.-Y. Kim, L.-S. Kim, and S.-H. Hwang, "An advanced contrast enhancement using partially overlapped sub-block histogram equalization," *IEEE Transactions on Circuits and Systems for Video Technology*, vol. 11, no. 4, pp. 475–484, 2001.

[4] S. G. Narasimhan and S. K. Nayar, "Contrast restoration of weather degraded images," *IEEE Transactions on Pattern Analysis and Machine Intelligence*, vol. 25, no. 6, pp. 713–724, 2003.
[5] S. Shwartz, E. Namer, and Y. Y. Schechner, "Blind haze separation," in *2006 IEEE Computer Society Conference on Computer Vision and Pattern Recognition (CVPR'06)*, vol. 2, 2006, pp. 1984–1991.
[6] J. Kopf, B. Neubert, B. Chen, M. Cohen, D. Cohen-Or, O. Deussen, M. Uyttendaele, and D. Lischinskii, "Deep photo: Model-based photograph enhancement and viewing," *ACM Trans. Graph.*, vol. 27, no. 5, pp. 116:1–116:10, 2008.
[7] R. T. Tan, "Visibility in bad weather from a single image," in *2008 IEEE Conference on Computer Vision and Pattern Recognition*, 2008, pp. 1–8.
[8] K. He, J. Sun, and X. Tang, "Single image haze removal using dark channel prior," *IEEE Transactions on Pattern Analysis and Machine Intelligence*, vol. 33, no. 12, pp. 2341–2353, 2011.
[9] R. Fattal, "Single image dehazing," *ACM Trans. Graph.*, vol. 27, no. 3, pp. 72:1–72:9, 2008.
[10] J. P. Tarel and N. Hautière, "Fast visibility restoration from a single color or gray level image," in *2009 IEEE 12th International Conference on Computer Vision*, 2009, pp. 2201–2208.
[11] G. Meng, Y. Wang, J. Duan, S. Xiang, and C. Pan, "Efficient image dehazing with boundary constraint and contextual regularization," in *2013 IEEE International Conference on Computer Vision*, 2013, pp. 617–624.
[12] R. Fattal, "Dehazing using color-lines," *ACM Trans. Graph.*, vol. 34, no. 1, pp. 13:1–13:14, 2014.
[13] Q. Zhu, J. Mai, and L. Shao, "A fast single image haze removal algorithm using color attenuation prior," *IEEE Transactions on Image Processing*, vol. 24, no. 11, pp. 3522–3533, 2015.
[14] I. Riaz, X. Fan, and H. Shin, "Single image dehazing with bright object handling," *IET Computer Vision*, vol. 10, no. 8, pp. 817–827, 2016.
[15] B. Cai, X. Xu, K. Jia, C. Qing, and D. Tao, "Dehazenet: An end-to-end system for single image haze removal," *IEEE Transactions on Image Processing*, vol. 25, no. 11, pp. 5187–5198, 2016.
[16] N. H. Kaplan, K. K. Ayten, and A. Dumlu, "Single image dehazing based on multiscale product prior and application to vision control," *Signal, Image and Video Processing*, 2017.
[17] C. Qin and X. Gu, "A single image dehazing method based on decomposition strategy," *Journal of Systems Engineering and Electronics*, vol. 33, no. 2, pp. 279–293, 2022.
[18] Z. Zhu, H. Wei, G. Hu, Y. Li, G. Qi, and N. Mazur, "A novel fast single image dehazing algorithm based on artificial multiexposure image fusion," *IEEE Transactions on Instrumentation and Measurement*, vol. 70, pp. 1–23, 2021.
[19] H. Ullah, K. Muhammad, M. Irfan, S. Anwar, M. Sajjad, A. S. Imran, and V. H. C. de Albuquerque, "Light-dehazenet: A novel lightweight cnn architecture for single image dehazing," *IEEE Transactions on Image Processing*, vol. 30, pp. 8968–8982, 2021.
[20] Y. Huang and X. Chen, "Single remote sensing image dehazing using a dual-step cascaded residual dense network," in *2021 IEEE International Conference on Image Processing (ICIP)*, 2021, pp. 3852–3856.
[21] J. Nunez, X. Otazu, O. Fors, A. Prades, V. Pala, and R. Arbiol, "Multiresolution-based image fusion with additive wavelet decomposition," *IEEE Transactions on Geoscience and Remote Sensing*, vol. 37, no. 3, pp. 1204–1211, 1999.
[22] K. He, J. Sun, and X. Tang, "Guided image filtering," *IEEE Transactions on Pattern Analysis and Machine Intelligence*, vol. 35, no. 6, pp. 1397–1409, 2013.
[23] S. G. Narasimhan and S. K. Nayar, "Vision and the atmosphere," *International Journal of Computer Vision*, vol. 48, no. 3, pp. 233–254, 2002.
[24] Y. Chai, H. Li, and M. Guo, "Multifocus image fusion scheme based on features of multiscale products and pcnn in lifting stationary wavelet domain," *Optics Communications*, vol. 284, no. 5, pp. 1146 – 1158, 2011.

Nur Huseyin Kaplan received his B. Sc., M. Sc, and Ph.D degrees in Electronics and Telecommunication Engineering from Istanbul Technical University, Turkey. He worked for TURKSAT A.Ş. as a specialist between 2005-2015. Since 2018, he is an Associate Professor at Electrical and Electronics Engineering Department with Erzurum Technical University, Turkey, where he teaches undergraduate/graduate level courses about signal and image processing. His primary research interests include digital signal and image processing.